

LSC-based electrode with high durability for IT-SOFCs

By Fei Zhao, Ranran Peng and Changrong Xia – Laboratory for Renewable Clean Energy, Department of Materials Science and Engineering, University of Science and Technology of China, Hefei, China

A highly stable electrode based on $\text{La}_{0.6}\text{Sr}_{0.4}\text{CoO}_{3-\delta}$ (LSC) has been developed for intermediate-temperature solid oxide fuel cells (IT-SOFCs). The electrode was prepared by impregnating LSC into a porous samaria-doped ceria (SDC, $\text{Sm}_{0.2}\text{Ce}_{0.8}\text{O}_{1.9}$) frame, which was deposited to an SDC electrolyte using screen-printing and co-firing techniques. The electrochemical properties of the composite electrode were investigated by impedance spectroscopy. High stability on thermal cycling was demonstrated for this composite electrode, although LSC and SDC have significant differences in thermal expansion. After 20 times of 500–800°C thermal cycles and 10 times of room-temperature-to-800°C thermal cycles, no increase in area specific resistance (ASR) was observed for such electrodes. In addition, improved performance was achieved with the impregnated composite electrode when compared with a conventional composite electrode prepared with a screen-printing technique.

Solid oxide fuel cells (SOFCs) are a forward-looking technology for highly efficient, environmentally friendly power generation. An SOFC is a multilayer structure consisting of at least three layers: an electrolyte layer sandwiched between an anode and a cathode layer. These layers have to show well adjusted thermal expansion behavior from room temperature to the operating temperature to avoid cracking and delamination during SOFC operation and thermal cycling.

Lanthanum cobaltite-based perovskites such as $\text{La}_{0.6}\text{Sr}_{0.4}\text{CoO}_{3-\delta}$ (LSC) are attractive materials as cathodes for intermediate-temperature (<800°C) solid oxide fuel cells (IT-SOFCs), because they have higher catalytic activity in the oxygen reduction reaction, higher oxide ion conductivity and higher electronic conductivity than lanthanum manganites, the classical cathode materials for SOFCs.^[1, 2] However, the thermal expansion coefficient (TEC) of LSC (i.e. $\sim 23 \times 10^{-6} \text{ K}^{-1}$) is much higher than those of typical SOFC electrolytes, such as yttria-stabilized zirconia (YSZ) and doped ceria electrolytes ($11\text{--}12 \times 10^{-6} \text{ K}^{-1}$). TEC mismatch between the electrolyte and the cathode will result in delamination at the cathode/electrolyte interface, and/or cracking of the electrolyte because of the stress developed on heating and cooling.^[3]

To minimize the potential problems associated with TEC mismatch, efforts have therefore been made to eliminate such TEC mismatch. For instance, by substituting Co with Fe and/or Ni in

LSC, a low TEC ($14.8 \times 10^{-6} \text{ K}^{-1}$) was achieved for $\text{La}_{0.8}\text{Sr}_{0.2}\text{Co}_{0.2}\text{Fe}_{0.8}\text{O}_{3-\delta}$, which is still much higher (>20%) than that of those electrolytes.^[4]

Unfortunately, the decrease in thermal expansion is usually accompanied by a decline in conductivity for the perovskites $\text{La}_{1-x}\text{Sr}_x\text{Co}_{1-y}\text{Fe}_y\text{O}_{3-\delta}$ with low cobalt contents. Specifically at 600°C, the conductivity of $\text{La}_{0.8}\text{Sr}_{0.2}\text{Co}_{0.2}\text{Fe}_{0.8}\text{O}_{3-\delta}$ is only 77 S/cm, whereas the conductivity is 1689 S/cm for $\text{La}_{0.8}\text{Sr}_{0.2}\text{CoO}_{3-\delta}$, and 2035 S/cm for $\text{La}_{0.6}\text{Sr}_{0.4}\text{CoO}_{3-\delta}$.^[4]

In general, the highest possible conductivity is desired to minimize the ohmic losses of the electrode. In another example, the electrolyte was incorporated into LSC to form a composite cathode.^[5, 6] Theoretically, the TEC of the composite cathode is smaller than that of LSC, but it is still larger than that of the electrolyte.

In addition, a new structure was proposed to modify the TEC mismatch. **Figure 1** shows the schematic diagram of this structure, in which the cathode consists of two continuous parts. One part is the so-called cathode frame, which is porous and joined to the electrolyte. The cathode frame has a rigid connection with the electrolyte substrate, and is made of the same material as the substrate. The other part is cobaltite-based perovskite particles embedded in the frame and joined to current-collecting materials. This structure was primarily reported for $\text{La}_{1-x}\text{Sr}_x\text{MnO}_{3-\delta}$ (LSM)-based composite

cathodes that were prepared with an ion-impregnation technique.^[7, 8]

The TEC decrease as an effect of this structure was first observed with an LSC–YSZ cathode by Huang et al.^[9] For example, a TEC as low as $12.6 \times 10^{-6} \text{ K}^{-1}$ was observed for a YSZ frame with 55 wt% LSC. However, performance losses with time were observed for the reported LSC–YSZ system. The degradation was likely to be due to the formation of insulating phases, such as SrZrO_3 .^[9]

In the present work, cathodes as shown in **Figure 1** were developed with samaria-doped ceria (SDC, $\text{Sm}_{0.2}\text{Ce}_{0.8}\text{O}_{1.9}$) as the electrolyte frame and LSC as the embedded component. Unlike YSZ, doped ceria is chemically stable with LSC at the operating temperature, and is often used as an interlayer for YSZ electrolyte-based SOFCs.

Strong bonding is formed between the porous SDC frame and the dense electrolyte substrate by co-firing the two layers. The strong bonding makes the porous cathode frame and dense electrolyte substrate essentially one unified piece, which will prevent delamination or cracking at the cathode/electrolyte interface during thermal cycling. Consequently, high resistance to thermal shock is expected for this cathode. This was confirmed in this work, with the degradation testing under abnormal conditions including thermal shock and thermal cycles.

Experimental

$\text{Sm}_{0.2}\text{Ce}_{0.8}\text{O}_{1.9}$ (SDC) powder used for substrates (electrolyte) was synthesized using an oxalate co-precipitation route and fired at 750°C for 2 h.^[10] Fine SDC powder used for slurry was prepared using a glycine-nitrate method.^[11] The powder was ball-milled with an ethyl cellulose binder and a terpineol-based solvent for 24 h to form a uniform SDC slurry.

The impregnated composite electrodes were prepared via a three-step process including substrate formation, frame coating and LSC

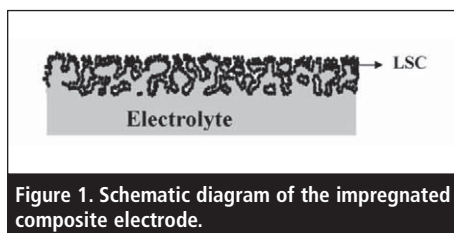


Figure 1. Schematic diagram of the impregnated composite electrode.

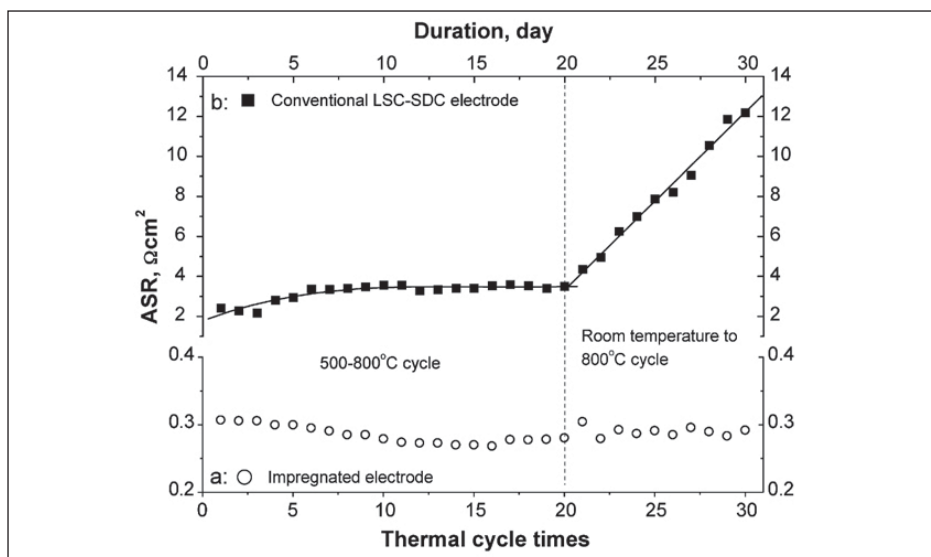


Figure 2. ASR at 600°C for (a) the impregnated electrode and (b) a conventional LSC-SDC electrode on thermal cycles.

impregnation. First, SDC substrates were prepared by dry-pressing SDC powder at 300 MPa. Second, the slurry was applied to both sides of the green SDC substrates to fabricate symmetric cells with a screen-printing technique. The substrates with the printed bi-layers were subsequently dried and co-fired in air at 1350°C for 5 h to form dense SDC substrates supporting porous SDC frames. The thicknesses for the porous SDC layer and dense SDC substrate were ~50 μm and ~0.8 mm, respectively, as measured with scanning electron microscopy (SEM). The area of the SDC frame was ~1.2 cm².

Finally, La_{0.6}Sr_{0.4}CoO_{3-δ} was embedded in the frame with an ion impregnation technique. To do this, La_{0.6}Sr_{0.4}Co(NO₃)_x nitrate solution was prepared by dissolving La(NO₃)₃·6H₂O, Sr(NO₃)₂ and Co(NO₃)₂·6H₂O in distilled water at a molar ratio of La:Sr:Co = 0.6:0.4:1, followed by adding glycine with a molar ratio of glycine to nitrates of 0.5. A few drops of the nitrate solution were placed on top of the porous layer frame and then infiltrated into the SDC pores by capillary force. To introduce sufficient amounts of LSC, the impregnation was repeated several times. The impregnated salts were finally heated to 800°C for 2 h to remove the nitrates and organics, and form a perovskite LSC.

The mass of the impregnated LSC before and after each impregnation cycle was measured, to estimate the LSC loading. In this work, 10 mg of LSC was impregnated into a 1 cm² porous SDC frame (50 μm thick) after 10 cycles. The final impregnated LSC-SDC electrode for measurement has a composition of 50 wt% LSC and 50 wt% porous SDC frame. For comparison, LSC-SDC composite (same weight fraction) electrode and pure LSC electrodes were prepared with the screen-printing technique and fired at 950°C for 2 h.

The phase structure of the impregnated LSC electrode was investigated using X-ray diffraction (XRD, D/Maxra X diffractometer with Cu K_α radiation). Microstructures were characterized using a JSM-6700F scanning electron microscope. Pt paste and Au wires were used for current collection in the symmetric electrodes. Two-probe measurements were conducted on the symmetric cells. Impedance spectra were measured on the symmetric cells under open-circuit conditions, with a frequency range from 0.01 Hz to 100 kHz and a 10 mV_{ac} perturbation, using a Zahner IM6e electrochemical station.

Results and discussion

Stability on thermal treatment

Shown in Figure 2a is the area-specific resistance (ASR) of the impregnated LSC-SDC electrode, measured at 600°C with the AC impedance technique on a symmetric cell, where the SDC electrolyte was ~0.8 mm thick. The ASR is typically used in the SOFC field to quantify all resistances associated with the electrodes which occur at the gas/electrode interface, within the bulk of the electrode, or at the electrode/electrolyte interface.^[12] The ASR data in this paper obtained in the Nyquist plot had been multiplied by 0.5 to account for the LSC-SDC electrodes.

The impedance measurement was conducted under open-circuit conditions for a period of 30 days, during which two stages of thermal cycling were applied to the electrode. The first stage was performed between 500 and 800°C with a heating and cooling rate of 5 degC/min. This stage proceeded with a fresh electrode, which was heated to 600°C and held for 2 h to measure the first impedance. After the measurement, the temperature was raised to 800°C and held for 30 min, followed by cooling to 500°C and holding at 500°C overnight. Finally the temperature was elevated to 600°C for the next measurement.

The thermal cycle was repeated 20 times, and almost no increase in ASR was observed. On the contrary, a slight decrease in ASR was recorded. The ASR was 0.306 Ωcm² for the first three measurements, and dropped to 0.281 Ωcm² after 20 thermal cycles. Therefore,

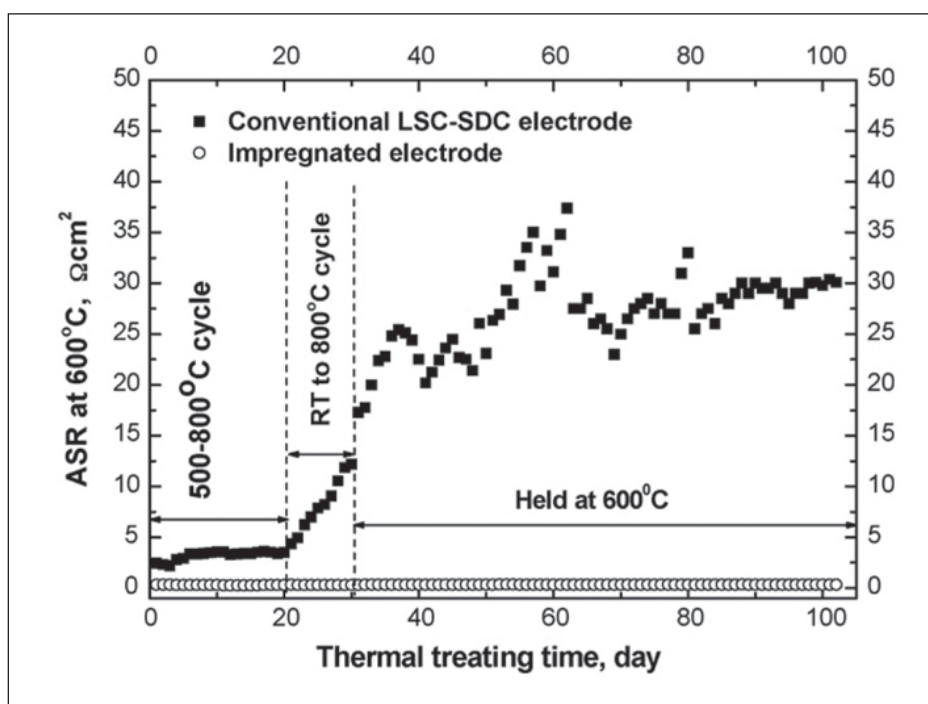


Figure 3. ASR at 600°C for the impregnated electrode and the conventional LSC-SDC electrode on thermal treatment.

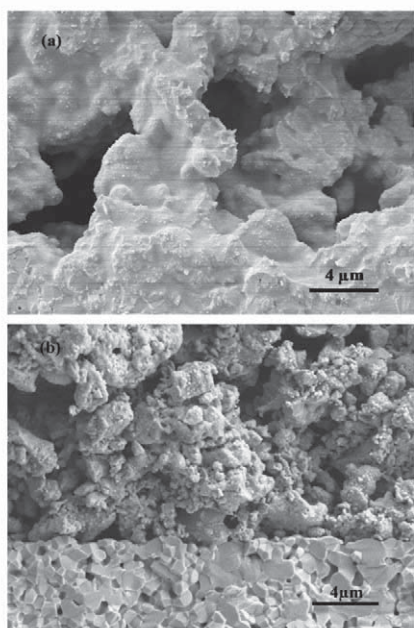


Figure 4. Cross-sectional microstructure views of (a) the impregnated electrode and (b) the conventional LSC-SDC electrode.

this impregnated composite cathode showed high stability on heating and cooling.

The stability is further examined in the subsequent thermal shock test. The second stage was performed at temperatures between 800°C and room temperature, at which the furnace was switched off to direct the shock test. The electrode temperature dropped to room temperature at a rate of up to 10 degC/min. The sample was further held at room temperature overnight, and heated to 600°C again for the impedance measurement. As shown in Figure 2a, the ASR is $0.290 \pm 0.007 \Omega\text{cm}^2$, and stays almost constant during the ten room-temperature-to-800°C cycles.

The advantages of this impregnated LSC-SDC electrode are distinctly illustrated by comparing the impregnated composite electrode with a conventional LSC-SDC (50 wt% LSC + 50 wt% SDC) composite electrode, which was prepared with the conventional screen-printing technique. As shown in Figure 2b, in the stage of the 500–800°C thermal cycling tests, the ASR of the conventional electrode increased from 2.42 to 3.50 Ωcm^2 . Therefore, in the first stage of thermal cycling, the ASR for the conventional LSC-SDC electrode increased by about 45%, compared to a slight decrease in ASR for the impregnated electrode.

The marked difference between the two electrodes was further observed at the second stage. The ASR for the conventional electrode increased from 3.50 to 12.2 Ωcm^2 , with an average increment of 0.93 Ωcm^2 per thermal cycle, while the ASR for the impregnated electrode stayed almost constant.

The stability of the impregnated electrode on thermal treatment is further shown in Figure 3,

where the electrode had been heat-treated for more than 2000 h. After 30 thermal cycles, the electrode was held at 600°C for more than three months. No obvious degradation was observed for the impregnated electrode, whereas the conventional electrode was highly unstable.

The high stability of this impregnated LSC-SDC electrode probably resulted from the special structure, which consisted of two continuous parts (the SDC and LSC phases). The major part is the so-called electrode frame (SDC phase), which is porous and joined to the SDC electrolyte. Figure 4a shows the cross-sectional microstructure of the impregnated electrode, which is supported on an SDC electrolyte substrate.

High-temperature sintering makes the electrode frame mechanically strong. The strong bonding makes the porous electrode frame and dense electrolyte substrate essentially one unified piece, which will prevent delamination or cracking at the electrode/electrolyte interface during thermal cycling. Consequently, high resistance to thermal shock is expected for such a designed composite electrode, compared to the conventional LSC-SDC electrode, which has poor binding at the electrode/electrolyte interface as shown in Figure 4b.

Electrode activity of impregnated composite electrode

It is encouraging that the impregnated LSC-SDC electrode showed not only superior thermal cycling performance, but also enhanced electrode activity compared with the conventional

LSC-SDC electrode. Comparing Figure 2a with 2b, it is clear that the ASR of the impregnated electrode is about 1/8 of the conventional one, indicating that the impregnated electrode possessed much higher electrochemical performance.

This advantage is further shown in Figure 5, which presents the ASR of the impregnated LSC-SDC electrode, the conventional LSC-SDC electrode, and a pure LSC electrode as a function of temperature. At 600°C, the ASR was only 0.29–0.31 Ωcm^2 for the impregnated electrode, while it was 2.2–2.6 Ωcm^2 for the conventional electrode, and 10–14 Ωcm^2 for the pure LSC electrode. Clearly, the ASR of the impregnated electrode is substantially lower than that of a single-phase LSC electrode (i.e. 1/5 to 1/10 of a conventional electrode), and is comparable to that of the best $\text{La}_{0.6}\text{Sr}_{0.4}\text{Co}_{0.2}\text{Fe}_{0.8}\text{O}_{3-\delta}$ -based composite systems with doped ceria as electrolytes.^[5, 6]

It should be mentioned that the impregnated electrode had a higher ASR than BICUVOX and $\text{Ba}_{0.5}\text{Sr}_{0.5}\text{Co}_{0.8}\text{Fe}_{0.2}\text{O}_{3-\delta}$ (BSCF)-based composites. The ASR was 0.055–0.071 Ωcm^2 at 600°C for BSCF composites using SDC as the electrolyte.^[13, 14] However, the stability of these cathodes is still questionable. Shown in Figures 6a and 6b are impedance spectra for the impregnated and conventional LSC-SDC electrodes. The two spectra are quite similar, implying the same oxygen reduction processes for the two electrodes.

The low ASR of the impregnated LSC-SDC electrode is also related to the microstructure of the composites. Figure 5a shows that the

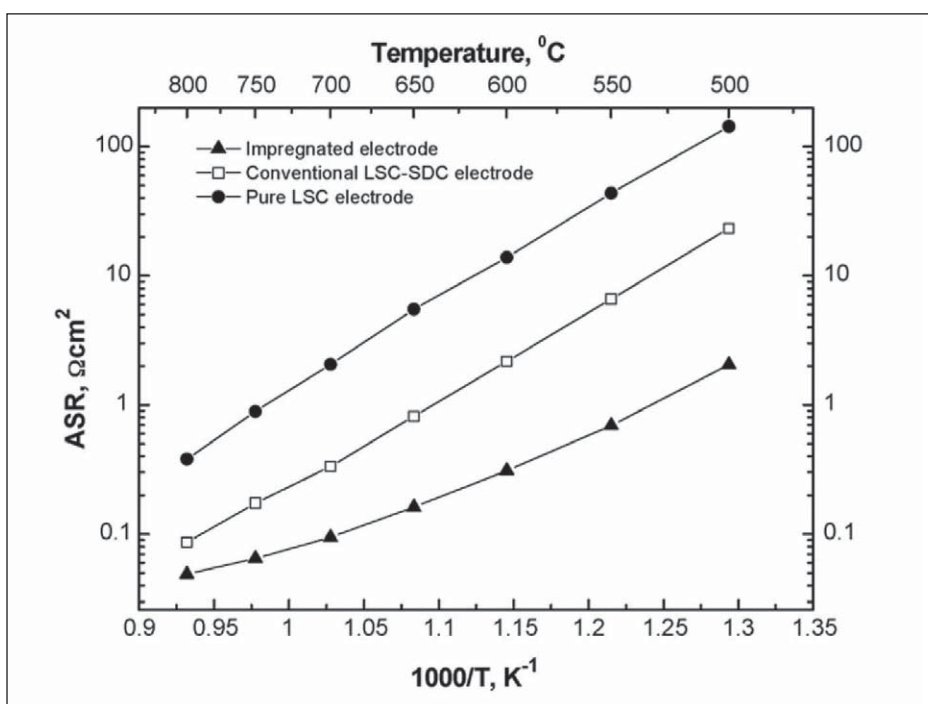


Figure 5. Temperature dependence of ASR for the impregnated electrode, the conventional LSC-SDC electrode, and a pure LSC electrode.

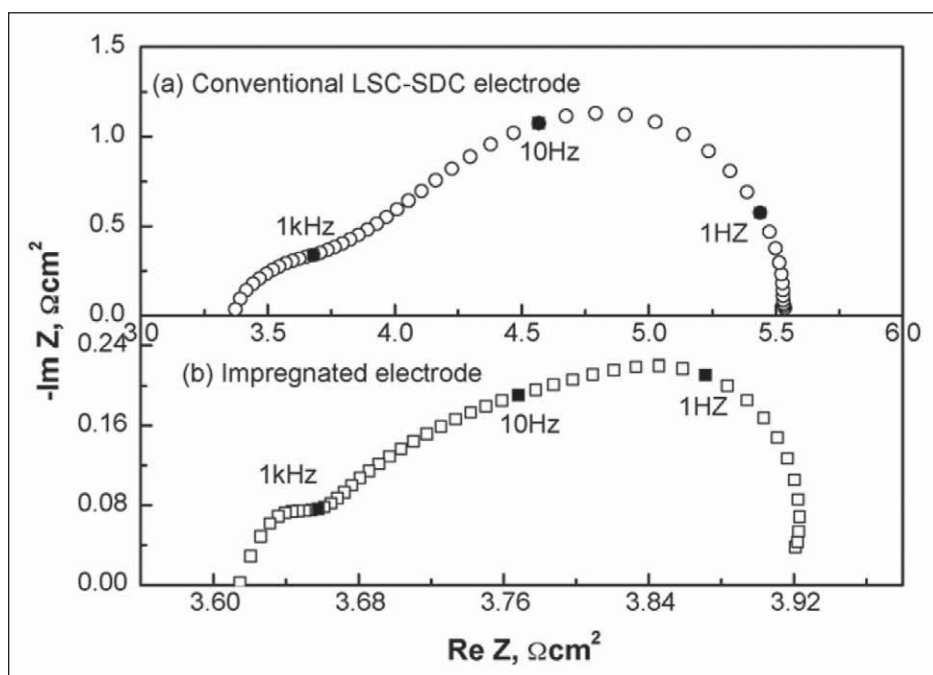
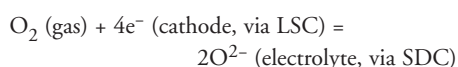


Figure 6. Impedance spectra at 600°C for (a) the conventional LSC-SDC electrode and (b) the impregnated electrode.

electrode frame (SDC) was well connected with the SDC electrolyte, and the fine LSC particles coated the SDC frame. This well connected structure makes a pathway for oxygen ion transport between the cathode (through the SDC frame) and the electrolyte (the SDC substrate), since SDC is an excellent oxide conductor.

It should be noted that the pathway was not only built across the electrode/electrolyte 'interface', but also within the electrode. Therefore, the length of the triple-phase boundaries (TPBs) was significantly extended. Consequently, cathodic activity is enhanced, since oxygen reduction takes place only at or near the triple-phase boundaries where oxygen ions can transport:



In a conventional cathode, it is difficult for oxygen ions to cross the interface. Furthermore, it is more difficult to travel within the cathode, since the oxygen ion pathway in the conventional cathode is built through the percolation of SDC particles. Therefore, the solid frame, which facilitates oxygen ion transport, may be one of the reasons for the reduced ASR of the impregnated electrode compared with the conventional composite electrode as well as the single-phase LSC electrode, as shown in Figure 5.

As shown in Figure 4a, fine particles of LSC were coated on the surface of the frame grains and also embedded in the frame pores. SEM observation under higher magnification (Figure 7) showed that the particles were ~50 nm

in size, and were likely formed by decomposition of impregnated $\text{La}_{0.6}\text{Sr}_{0.4}\text{Co}(\text{NO}_3)_x$ nitrate solution. This size is generally much smaller than that of particles in a conventional electrode. The latter has to be sintered at a temperature higher than 900°C to obtain a reasonable bonding strength between the electrode and electrolyte.

The small LSC particles as cathodic catalyst are believed to accelerate the rate of oxygen surface exchange, which is a critical step for oxygen reduction at the cathode, and also extend the length of the TPBs. Therefore, small LSC particles should be another reason for the lower ASR of the impregnated electrode.

Conclusions

The present study has demonstrated that the $\text{La}_{0.6}\text{Sr}_{0.4}\text{CoO}_{3-\delta}$ -impregnated electrode shows remarkable performance. The high resistance to thermal cycling and thermal shock has been achieved despite significant thermal expansion coefficient mismatch between the $\text{La}_{0.6}\text{Sr}_{0.4}\text{CoO}_{3-\delta}$ catalyst and $\text{Sm}_{0.2}\text{Ce}_{0.8}\text{O}_{1.9}$ electrolyte. In addition, a very low area-specific resistance has been achieved. These results imply that a reliable electrode with high thermal resistance and high performance has been developed for intermediate-temperature solid oxide fuel cells.

Acknowledgments

This work was supported by the National Nature Science Foundation of China under award Nos. 50372066 and 50332040.

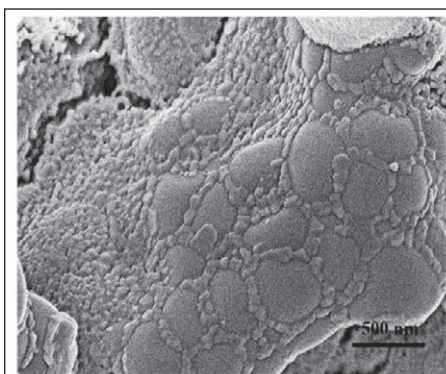


Figure 7. Cross-sectional microstructure view of LSC particles coated on SDC grains.

This article is based on a paper published recently in *Materials Research Bulletin* **43**(2) 370–376 (5 February 2008) [DOI: 10.1016/j.materresbull.2007.03.006].

References

1. S.B. Adler: Factors governing oxygen reduction in solid oxide fuel cell cathodes, *Chem. Rev.* **104**(10) (2004) 4791–4844.
2. R.M. Ormerod: Solid oxide fuel cells, *Chem. Soc. Rev.* **32** (2003) 17–28.
3. N.Q. Minh and T. Takahashi: Science and technology of ceramic fuel cells (Elsevier, Amsterdam, 1995) 117–146.
4. A. Petric, P. Huang and F. Tietz: Evaluation of La–Sr–Co–Fe–O perovskites for solid oxide fuel cells and gas separation membranes, *Solid State Ionics* **135**(1–4) (2000) 719–725.
5. V. Dusastre and J.A. Kilner: Optimisation of composite cathodes for intermediate temperature SOFC applications, *Solid State Ionics* **126**(1–2) (1999) 163–174.
6. E.P. Murray, M.J. Sever and S.A. Barnett: Electrochemical performance of (La,Sr)(Co,Fe)O₃–(Ce,Gd)O₃ composite cathodes, *Solid State Ionics* **148**(1–2) (2002) 27–34.
7. Y. Huang, J.M. Vohs and R.J. Gorte: Characterization of LSM-YSZ composites prepared by impregnation methods, *J. Electrochem. Soc.* **152**(7) (2005) 1347–1353.
8. T.Z. Sholkapper, C. Lu, C.P. Jacobson, S.J. Visco and L.C. De Jonghe: LSM-infiltrated solid oxide fuel cell cathodes, *Electrochem. Solid-State Lett.* **9**(8) (2006) 376–378.
9. Y. Huang, K. Ahn, J.M. Vohs and R.J. Gorte: Characterization of Sr-doped LaCoO₃-YSZ composites prepared by impregnation methods, *J. Electrochem. Soc.* **151**(10) (2004) 1592–1597.
10. R.R. Peng, C.R. Xia, D.K. Peng and G.Y. Meng: Effect of powder preparation on (CeO₂)_{0.8}(Sm₂O₃)_{0.1} thin film properties by screen-printing, *Mater. Lett.* **58**(5) (2004) 604–608.

11. R.R. Peng, C.R. Xia, Q.X. Fu, G.Y. Meng and D.K. Peng: Sintering and electrical properties of $(\text{CeO}_2)_{0.8}(\text{Sm}_2\text{O}_3)_{0.1}$ powders prepared by glycine–nitrate process, *Mater. Lett.* **56**(6) (2002) 1043–1047.
12. S.P. Jiang: A review of wet impregnation – An alternative method for the fabrication of high performance and nano-structured electrodes

- of solid oxide fuel cells, *Mater. Sci. Eng. A* **418**(1–2) (2006) 199–210.
13. Z.P. Shao and S.M. Haile: A high-performance cathode for the next generation of solid-oxide fuel cells, *Nature* **431** (2004) 170–173.
14. C. Xia and M. Liu: Novel cathodes for low-temperature solid oxide fuel cells, *Adv. Mater.* **14**(7) (2002) 521–523.

Contact: Professor Changrong Xia, Laboratory for Renewable Clean Energy, Department of Materials Science & Engineering, University of Science and Technology of China, Hefei, Anhui 230026, China. Tel: +86 551 360 7475, Fax: +86 551 360 6689, Email: xiacr@ustc.edu.cn, Web: mse.ustc.edu.cn/en/

For more on the *Materials Research Bulletin*: www.sciencedirect.com/science/journal/00255408

Research Trends

Review of polymer electrolyte membranes for DMFCs

V. Neburchilov et al.: *J. Power Sources* **169**(2) 221–238 (20 June 2007).
DOI: 10.1016/j.jpowsour.2007.03.044

Review of direct liquid-feed fuel cells: thermodynamic and environmental concerns

U.B. Demirci: *J. Power Sources* **169**(2) 239–246 (20 June 2007).
DOI: 10.1016/j.jpowsour.2007.03.050

Ni/YSZ and Ni–CeO₂/YSZ SOFC anodes prepared by impregnation

J. Qiao et al.: *J. Power Sources* **169**(2) 253–258 (20 June 2007).
DOI: 10.1016/j.jpowsour.2007.03.006

Novel H₃PO₄/Nafion–PBI composite membrane for enhanced durability of high-temperature PEMFCs

Y. Zhai et al.: *J. Power Sources* **169**(2) 259–264 (20 June 2007).
DOI: 10.1016/j.jpowsour.2007.03.004

Effects of anode and electrolyte microstructures on SOFC performance

S.-D. Kim et al.: *J. Power Sources* **169**(2) 265–270 (20 June 2007).
DOI: 10.1016/j.jpowsour.2007.03.046

Innovative gas diffusion layers and their water removal characteristics in PEMFC cathode

K. Jiao and B. Zhou: *J. Power Sources* **169**(2) 296–314 (20 June 2007).
DOI: 10.1016/j.jpowsour.2007.03.042

DOI numbers

The digital object identifier (DOI) is a unique, permanent character string used to link to electronic documents. To resolve a DOI, go to the website <http://dx.doi.org>, enter the entire DOI citation (for example, 10.1016/j.ssi.2007.04.002) in the box, and click 'Go'.

PEM fuel cell mini power unit for portable electronic devices

F. Urbani et al.: *J. Power Sources* **169**(2) 334–337 (20 June 2007).
DOI: 10.1016/j.jpowsour.2007.03.049

Review of metal hydride materials for solid hydrogen storage

B. Sakintuna et al.: *Int. J. Hydrogen Energy* **32**(9) 1121–1140 (June 2007).
DOI: 10.1016/j.ijhydene.2006.11.022

Microstructure control of SOFC cathodes using self-organizing behavior of LSM/ScSZ composite powder prepared by spray pyrolysis

A. Hagiwara et al.: *Solid State Ionics* **178**(15–18) 1123–1134 (June 2007).
DOI: 10.1016/j.ssi.2007.05.005

Review of catalysts for direct ethanol fuel cells

E. Antolini: *J. Power Sources* **170**(1) 1–12 (30 June 2007).
DOI: 10.1016/j.jpowsour.2007.04.009

Cross-linked sulfonated fluorene-containing poly(arylene ether ketone) for PEM

F.C. Ding et al.: *J. Power Sources* **170**(1) 20–27 (30 June 2007).
DOI: 10.1016/j.jpowsour.2007.03.068

Ammonia-fueled SOFC with BaCe_{0.9}Nd_{0.1}O_{3–δ} thin electrolyte prepared with suspension spray

K. Xie et al.: *J. Power Sources* **170**(1) 38–41 (30 June 2007).
DOI: 10.1016/j.jpowsour.2007.03.059

La(Ni,Fe)O₃ as SOFC cathode material with high tolerance to chromium poisoning

Y.D. Zhen et al.: *J. Power Sources* **170**(1) 61–66 (30 June 2007).
DOI: 10.1016/j.jpowsour.2007.03.079

Review of current development and applications of micro fuel cells

A. Kundu: *J. Power Sources* **170**(1) 67–78 (30 June 2007).
DOI: 10.1016/j.jpowsour.2007.03.066

Comparative study of CCMs and hot-pressed MEAs for PEMFCs

H. Tang et al.: *J. Power Sources* **170**(1) 140–144 (30 June 2007).
DOI: 10.1016/j.jpowsour.2007.03.062

Refractory alkaline earth silicate sealing glasses for planar SOFCs

Y.-S. Chou et al.: *J. Electrochem. Soc.* **154**(7) B644–651 (July 2007).
DOI: 10.1149/1.2733868

Membrane degradation mechanisms in PEMFCs

V.O. Mittal et al.: *J. Electrochem. Soc.* **154**(7) B652–656 (July 2007).
DOI: 10.1149/1.2734869

Chemical stability of ferritic alloy interconnect for SOFCs

K. Ogasawara et al.: *J. Electrochem. Soc.* **154**(7) B657–663 (July 2007).
DOI: 10.1149/1.2735919

Transition metal oxides as DMFC cathodes without platinum

Y. Liu et al.: *J. Electrochem. Soc.* **154**(7) B664–669 (July 2007).
DOI: 10.1149/1.2734880

Study of SOFC anode functional layers based on ceria in YSZ

M.D. Gross et al.: *J. Electrochem. Soc.* **154**(7) B694–699 (July 2007).
DOI: 10.1149/1.2736647

Development of improved devitrifiable SOFC sealing glass

M.D. Dolan and S.T. Mixture: *J. Electrochem. Soc.* **154**(7) B700–711 (July 2007).
DOI: 10.1149/1.2737664

Sulfated zirconia as support of Pt catalyst for PEMFCs

Y. Suzuki et al.: *Electrochem. & Solid-State Letters* **10**(7) B105–107 (July 2007).
DOI: 10.1149/1.2730625